Electrochemical Behavior of Alloys for Fixed Partial Denture

Pascal de March, Patrice Berthod

▶ To cite this version:

Pascal de March, Patrice Berthod. Electrochemical Behavior of Alloys for Fixed Partial Denture. Open Corrosion Journal, Bentham Open, 2009, 2, pp.8 - 16. hal-02321225

HAL Id: hal-02321225
https://hal.archives-ouvertes.fr/hal-02321225

Submitted on 21 Oct 2019

Electrochemical Behavior of Alloys for Fixed Partial Denture

Pascal De March[1,2] and Patrice Berthod[*,1]

[1]*Solid Mineral Chemistry Laboratory (LCSM) CNRS, Faculty of Science and Techniques, Nancy-University, B.P. 239, 54506 Vandoeuvre-lès-Nancy, France*

[2]*Faculty of Dentistry, Department of Prosthodontics, Nancy-University, 96 Avenue De Lattre de Tassigny, BP 50208, 54004 Nancy Cedex, France*

Abstract: The electrochemical behaviors of eight parent alloys and four post-solder alloys used in dental prostheses were specified in a (pH=7.4; [NaCl]=9g/L)-aqueous solution at 37°C. For each alloy, the free potential was followed during two hours, and a cyclic polarization between the cathodic domain and the solvent's oxidation was performed. The galvanic corrosion between each parent alloy and its usual post-solder was also studied. The free potentials stay in the immunity domain of the alloy's base-elements (precious metals) or in their passivation domain (nickel, chromium). A relatively strong oxidation of the alloys is possible only for high values of applied potential. Corrosion of the noblest alloys is almost inexistent. It occurs for the nickel-base alloys but it is very slow. Most of the elements present can be oxidized, but only for high potentials which cannot be really achieved by dissolved oxygen. Galvanic corrosion can occur between the parent alloy and the post-solder alloy in some cases.

Keywords: Dental alloy, electrochemical measurement, corrosion behavior, artificial saliva.

INTRODUCTION

The realization of frameworks for fixed partial denture (FPD) often involves the use of more or less noble metallic alloys and their assemblage by soldering. The latter is called pre-ceramic soldering or post-ceramic soldering, this depending on the step of the fabrication of the prostheses at which this soldering is realized. Soldering is well used to correct distortion of the framework which occurs during the casting process [1], to improve the seating accuracy [2] and to correct a possible movement of teeth before prosthesis cementation [3]. The solder joint is often the weakest part of a fixed partial denture [4, 5]. While some defects can be due to the process of fabrication [6], others can appear during the use of the prosthesis in the mouth, because of corrosion by saliva which can generate additional cavities on alloy surface. Indeed, the metallic framework may partly remain exposed to the buccal milieu, notably a part of the parent alloy and the post-ceramic solder which is not covered by ceramic. These are the reasons why the individual behaviors of main alloy of the framework and of the post-solder alloys in contact with saliva need to be better known, as well as the behavior of this parent alloy coupled with its usual post-solder.

The purpose of this article is first to specify the separate behaviors of the parent alloy and of the post-ceramic solder, and second to study the possible galvanic corrosion which could be due to the association of the two materials, by using electrochemical techniques. The electrolyte used in this study, is characterized by a NaCl concentration of 9 g/L and a pH equal to 7.4, and it simulates the oral environmental conditions. This solution was already used in several studies concerning the electrochemical characterization of corrosion of dental alloys, even by using impedance spectroscopy [7], but generally for alloys which are different from ours.

MATERIALS AND METHODOLOGY

Eight alloys were studied here: five alloys called "High Noble" particularly rich in precious metals, one "Noble" alloy (less rich in precious metals than the first ones) and two "Predominantly Base" alloys (which are based on nickel and chromium), which are denominations according to the Identalloy norm. Their corresponding post-solder alloys have been also investigated. All these commercial alloys and solders are marked by the same manufacturer (Ivoclar-Vivadent, Schaam, Lichtenstein). Table **1** indicates, the manufacturer compositions of the alloys, of the solders and the alloy-solder associations as reported by the manufacturer.

Synthesis of the Parent Alloys and Post-Solder Alloys

Each parent alloy was investment cast following a method which was already described in another work [6], but which can be summarized as follows. The samples for study were realized by injection of a pattern resin in a machined metallic mould. Several samples of 10x10x1 mm^3 were invested together for each alloy. All castings were synthesized with 100% new alloy (no re-casting) using a casting machine with centrifugal arm and a gas-oxygen torch. All samples were separated from the cast-rod with a diamond separated disk on hand-piece. For each alloy, one sample of 10x10x1 mm^3 was cut into four equal pieces (5x5x1 mm^3) with a diamond blade on a slow-speed precision saw (Isomet 5000, Buelher). Each sample was blasted with alumina 50 μm - powder. Thereafter, all alloys underwent a heat treatment, following the thermal cycle required for the respective

*Address correspondence to this author at the Solid Mineral Chemistry Laboratory (LCSM) CNRS, Faculty of Science and Techniques, Nancy-University, B.P. 239, 54506 Vandoeuvre-lès-Nancy, France; E-mail: patrice.berthod@lcsm.uhp-nancy.fr

Table 1.   Designation and Chemical Compositions of the Studied Alloys (in Weight Percent, Manufacturer's Data)

Elements	Au	Pt	Pd	Ag	Ga	In	Re	Ru	Sn	Zn	Others	
High Noble Alloys (for Which Au+Pt+Pd > 60%)												
IPS dSIGN98	85.9	12.1	-	-	-	<1.0	-	-	-	2.0	In<1 Fe<1 Ta<1	Ir<1 Mn<1
Aquarius Hard	86.1	8.5	2.6	-	-	1.4	-	<1.0	-	-	Fe<1 Ta<1	Li<1
IPS dSIGN91	60.0	-	30.55	-	1.0	8.4	<1.0	<1.0	-	-	-	
Lodestar	51.5	-	38.5	-	1.5	8.5	<1.0	<1.0	-	-	-	
W	54.0	-	26.4	15.5	-	1.5	<1.0	<1.0	2.5	-	Li<1	
Noble Alloy (Containing Au+Pt+Pd)												
IPS dSIGN59	-	<1.0	59.2	27.9	-	2.7	<1.0	<1.0	8.2	1.3	Li<1	
Predominantly Base Alloys (Containing Less than 25% Au+Pt+Pd)												
Elements	Ni	Cr	Mo	Al	Si	W	Others					
4all	61.4	25.7	11.0	<1	1.5		Mn<1					
Pisces Plus	61.5	22.0	-	2.3	2.6	11.2	Mischmetal<1					
Post-Solder Alloy												
Elements	Au	Ag	Cu	Ga	In	Sn	Zn	Used with …				
.650 Gold Solder	65.0	13	19.6	2.0	-	-	<1.0	dSIGN98				
.615 Fine Solder	61.3	13.1	17.4	-	7.6	-	<1.0	dSIGN91, d59, Lodestar				
.585 Fine solder	58.5	16.0	18.0	7.2	-	-	<1.0	Aquarius Hard				
LFWG	56.1	27.4	-	-	<1.0	<1.0	15.8	W, Pisces Plus, 4ALL				

oxidation heat treatment of each alloy, which was done in a ceramic oven (Programat X1, Ivoclar Vivadent). All thermal cycles were realized according to the manufacturer's advices for ceramic (IPS dSIGN ceramic, Ivoclar Vivadent).

For each post-solder electrode an entire solder rod (supplied by the manufacturer) was melt using a butane-oxygen blowtorch in a borax-vitrified crucible, which led to a half ball-like ingot of around 1 gram. Each ingot was sand-blasted and steam-cleaned. Thereafter, the heat treatment indicated by the manufacturer especially for this post-solder alloy was applied to the ingot in the ceramic oven.

Realization of the Electrodes and Electrochemical Measurements

To obtain the electrodes needed for the electrochemical experiments, each sample of parent alloy or of post-solder alloy was tin-soldered to a plastic-covered copper wire. The sample was then embedded in a cold resin (Araldite CY230 +Strengthener Escil HY956) in order to totally cover the alloy-wire junction. It was thereafter polished first with SiC paper from 80 to 1200 grid under water, and finished with 1μm diamond paste. The area of polished alloy exposed to the solvent is a square of about 25 mm² for the parent alloys'

electrodes, and a disk of around 35 mm² for the post-solder alloys. It was possible to examine the microstructures of the alloys in the electrodes since the wire emerged from the side of the embedded part, which allowed placing them in the Philips XL30 Scanning Electron Microscope (SEM) for their observation in Back Scattered Electrons mode (BSE).

The apparatus which was used here was composed of a potentiostat/galvanostat 263A of Princeton Applied Research (driven by the EGG/Princeton model 352 software) and a cell in which the electrolytic solution is maintained at 37 ± 1°C by the external flow of a heated liquid generated by a Julabo F32 device. In this cell, three electrodes, the Working Electrode (the studied alloy), a platinum Counter Electrode and a Saturated Calomel Electrode (potential reference, 241.5mV/Normal Hydrogen Electrode), were immersed in an (37°C; pH=7.4; 9g/L NaCl) aqueous solution prepared from distilled water, pure NaCl and HCl for adjustment of pH.

For each parent or post-solder alloy, two experiments were run successively:

-       follow-up of the open circuit potential E_{ocp} over 2 hours,

- cyclic polarization: increase in potential from E_{ocp} - 150 mV up to 1.225 V at 1 mV/s, followed by a decrease in potential down to the initial value (E_{ocp} - 150 mV).

For each parent alloy associated to its usual post-solder alloy, in situation of galvanic corrosion, during one hour:

- follow-up of the common potential of both the parent alloy and post-solder alloy electrodes together electrically connected, versus the SCE potential

- follow-up of the current density between the two electrodes (intensity divided by the anodic surface).

The results files were treated with an Excel (Microsoft, USA) mask especially built, in which the data for pH=7.4 of all the Pourbaix's diagrams [8] of the different elements present in the alloys were included for an easy comparison between the recorded curves and the different domains for the elements. The use of Pourbaix's diagrams, which supposes that thermodynamic equilibrium is established (what is not really the case here) will nevertheless give useful indications about reactions.

RESULTS

Microstructures of Alloys in the Electrodes

The alloys often display two distinct phases since, in seven cases on eight, there are simultaneously a main phase (the matrix) and a dispersed phase (precipitates). The precipitates are either clearer or darker than matrix when microstructure is examined using the SEM in BSE mode. The microstructures of the parent alloys microstructures and of the post-ceramic solders are illustrated by (SEM, BSE) micrographs in Fig. (**1**). In the alloys dSIGN 98, dSIGN91, Aquarius Hard and Lodestar, there are precipitates which are darker than matrix, since heavy elements (Au, Pt) are more present in matrix than in these precipitates, as shown by WDS microanalysis [6]. On the contrary, precipitates are clearer than matrix in the cases of 4All and Pisces Plus since they contain molybdenum or tungsten in a Ni-Cr matrix. In addition, the Pisces Plus alloy clearly displays a dendritic structure which can be attributed to a chemical heterogeneity due to segregation during solidification. The W alloy is the sole of the eight to be obviously monophased.

The post-solder alloys .585, .615 and .650 seem to be almost monophased, while, on the contrary, the LFWG alloy is clearly composed of two distinct phases with similar surface fractions.

Preliminary Study of the Electroactivity of the Solution

In the three electrodes-apparatus, a second platinum counter electrode was used instead of the working electrode (i.e. the studied alloy), in order to specify the electroactivity of the solution. By performing the two types of experiments which were applied to the parent or post-solder alloys themselves, one obtained the results displayed as graphs in Fig. (**2**). In that ones, it appeared that, after a slight initial decrease, the free potential became stabilized at about 200 mV/NHE, of course in the immunity domain of platinum. The second graph presents the cyclic polarization curve from the cathodic domain (E_{ocp} - 150mV, i.e. about +30 mV/NHE) towards the anodic domain (up to about 1,500 mV/NHE),

and return down to the initial value of the potential in the cathodic domain. The E_{ocp} potential in the first part of the curve (increasing potential) is about 180 mV/NHE while it became about 450 mV/NHE in the second part of the curve (decreasing potential). The increasing-potential part of the anodic curve presents an accelerated increase in the current density, which corresponds to the oxidation of Pt into $Pt^{II}(OH)_2$ then $Pt^{IV}O_2$, followed by the oxidation of the solvent about 0.5V over the O_2/OH^- potential. The E(I=0) potential obtained on the first part of the curve corresponds to the O_2/OH^- equilibrium (1/2 x O_2 + n x e + H^+ ↔ OH^- with n=2), as confirmed by the values of the Tafel coefficients $\beta a \approx \beta c \approx 60$mV/decade (i.e. n=2 effectively) which were calculated according to the Tafel method. The E(I=0) potential in the decreasing-potential part of the polarization curve, which is higher than the first one, corresponds now to the $Pt^{II}(OH)_2/Pt^0$ equilibrium.

Study of the Electrochemical Behavior of the High Noble Alloys

To simplify, all the High Noble alloys (dSIGN98, Aquarius Hard, dSIGN91, Lodestar and W), which are based on gold, led to similar global behaviors (Fig. **3a** and Table **2**). However they need to be separated in two groups. dSIGN98 and Aquarius Hard remain at high levels of free potential (100 and 400 mV/NHE) before the cyclic polarization runs. These potentials are then in the immunity domain of the base element of the two alloys, i.e. Au, as well as in the one of either Pt and/or Pd, the other noble elements which are also present. Concerning the other elements (Zn and In) the potentials correspond to their passivation domains, which means that, if they would be concerned by corrosion, they would be oxidized into solid (oxide or hydroxide) formed on surface. This can be more or less the case for the two alloys, since the lightest elements in their compositions obviously belong to the precipitates existing together with matrix. The polarization curves of these two first alloys present almost the same features. As illustrated in Fig. (**3a**) with the case of dSIGN98, the first part of the curve (with an increasing potential) is characterized by a E_{ocp} potential which is in the immunity domain of gold, platinum and/or palladium (and also in the passivation domains of Zn or In). In the anodic part, the potential increases without a real increase of the anodic current density, except when the potential becomes higher than the $Au^0/Au^{III}(OH)_3$ frontier. Indeed, Au becomes then oxidized, seemingly in Au^{III} ions (active state) just before falling in a passive state probably obtained by the development of a continuous layer of $Au(OH)_3$. About 0.5V above the O_2/OH^- frontier (i.e. above the band of kinetic immunity of water), the solvent begins to be oxidized itself. Thereafter, the decreasing potential part of the cyclic polarization curve is characterized by a new E_{ocp} potential, higher than the first one since it now corresponds to the Au^{III}/Au^0 equilibrium. The same type of behavior was met for the three other High Noble alloys (dSIGN91, Lodestar and W) before the cyclic polarization run, with a more or less high level of free potential which however remained in the immunity domains of Au, Pt, Pd and Ag, as well as in the passivation domains of In, Ga and Sn. It was also true for the increasing-potential part of the polarization curve, but differences became apparent in its second part since, in addition to the (I=0) peak of the Au^{III}/Au^0 equilibrium, there are also other peaks either situated above the latter (dSIGN91, Lodestar, W)
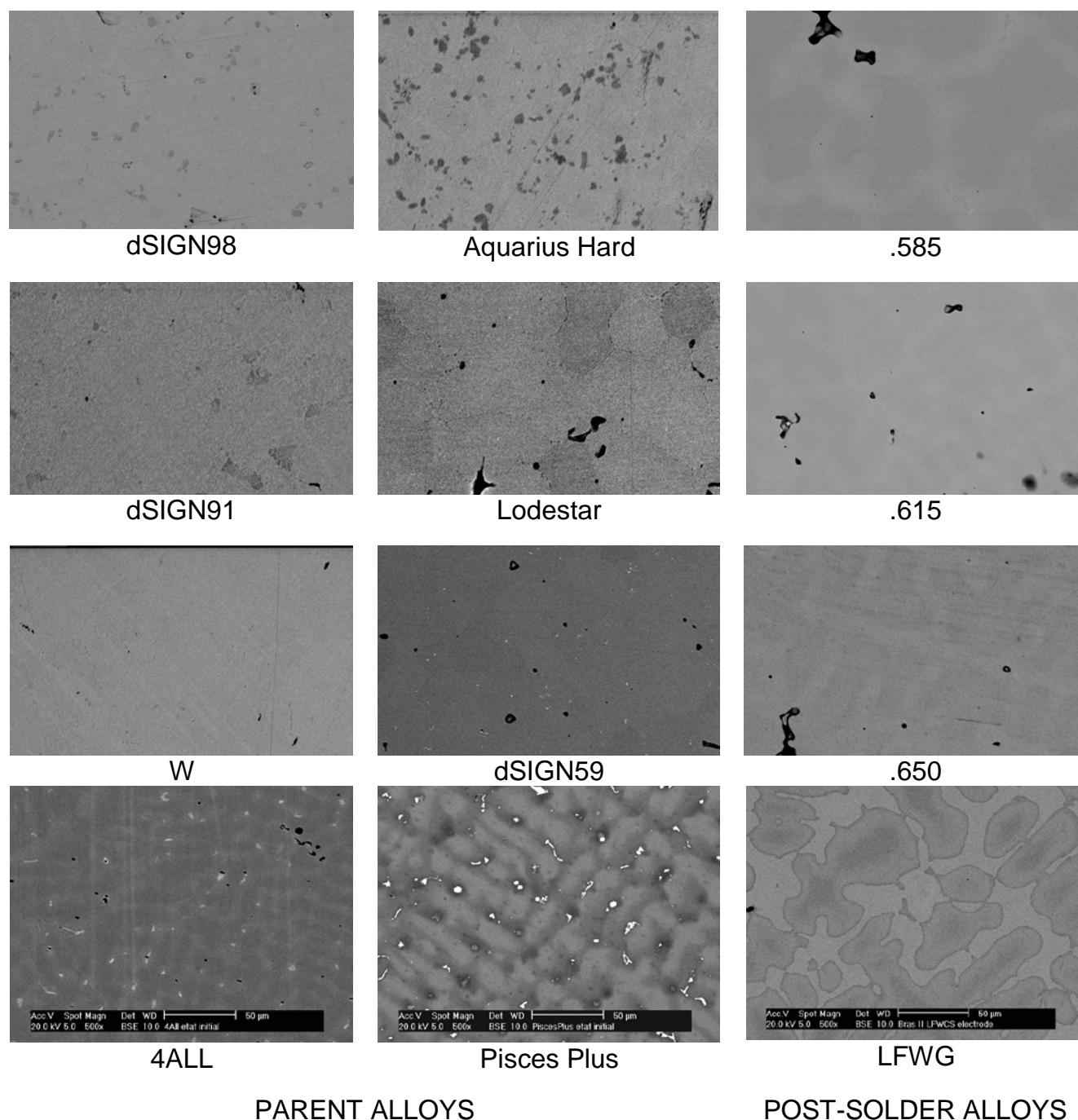
Fig. (1). Microstructures of the twelve electrodes as seen with the SEM in BSE mode (scale of all micrographs given in the bottom ones only).

or below (Lodestar only). These other peaks seems corresponding to the different equilibriums for palladium ($Pd^{IV}(OH)_4/Pd^{II}(OH)_2$ and $Pd^{II}(OH)_2 /Pd^0$) in the case of the Pd-rich Lodestar alloy, and for Pd and Ag ($Pd^{IV}(OH)_4/Pd^{II}(OH)_2$ and $Ag^{II}O / Ag^I_2O$) in the case of the Pd-rich Ag-containing W alloy.

Study of the Electrochemical Behavior of the Noble and Predominantly Base Alloys

The Noble Pd-based dSIGN59 alloy displays a behavior which is similar to the Au-richest High Noble alloys (Fig. **3b**

and Table **3**), since the potential remains in the immunity domains of both Pd and Ag (and the passivation domains of Sn, In and Zn). However the potential is a little lower than for the High Noble alloys. The cyclic polarization curve shows a small anodic peak (oxidation of Pd^0 into Pd^{II} ions) followed by a passivation plateau ($Pd^{II}(OH)_2$), then a new oxidation of $Pd^{II}(OH)_2$ into $Pd^{IV}(OH)_4$ (almost simultaneously with the oxidation of Ag^0 in Ag^I_2O, in $Ag^{II}O$ and in $Ag^{III}_2O_3$) and finally the oxidation of the solvent. No additional peaks appeared in the decreasing-potential part of the

curve, which displays a new free potential that is more than 200 mV higher than the one of the increasing-potential part.
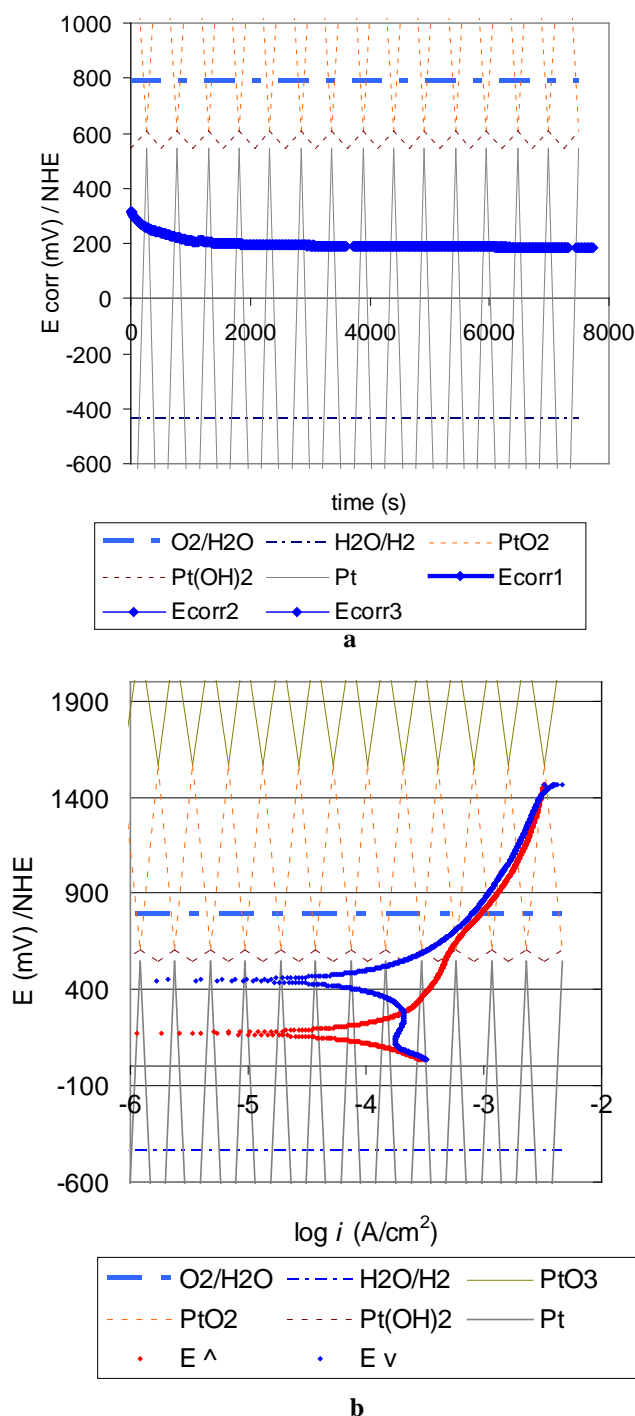

Fig. (2). Follow-up of the free potential of a Pt electrode (**a**) and cyclic polarization of Pt (**b**), both in the (pH=7.4; 9g/L) aqueous solution of the study.

For the two PB alloys, 4ALL and Pisces Plus, the free potentials recorded before cyclic polarization are in the passivation domain of the alloys: $Ni^{II}(OH)_2$ and $Cr^{III}(OH)_3$ (but MoO_4^{2-} ions) for 4ALL and $Ni^{II}(OH)_2$, $Cr^{III}(OH)_3$ and WO_3 for Pisces Plus. Their potentials are sensibly lower than for the precedent alloys. If the free potential of 4ALL remains

slightly lower than for Pisces Plus, the reason can be that the Pisces Plus potential raised just after immersion and stabilized at several tens millivolts. Their two polarization curves (Pisces Plus in Fig. (**3c**)) are simpler than for most of the precedent alloys, since only one E_{ocp} peak can be seen on the increasing-potential part and only one too on the decreasing-potential part. If the new E_{ocp} potential after cyclic polarization is above the initial one for the 4ALL alloy, the two E_{ocp} potentials before and after cyclic polarization are equals in the case of Pisces Plus.

Study of the Electrochemical Behavior of the Post-Solder Alloys

In all cases the free potential before cyclic polarization is in the immunity domains of both gold and silver (Fig. **3d** and Table **4**), with sensibly the same values between the different post-solder alloys. It is also in the passivation domain of Ga, In and Zn and seems close to the equilibrium potential between $Cu^{II}(OH)_2$ and Cu^{I}_2O when the studied post-solder contains copper. These potentials are also rather close to the free potentials observed for the High Noble parent alloys. When the polarization cycle is applied, there are oxidation processes on the potential-increasing part which finished with the oxidation of gold and of the solvent, like for the most of parent alloys. On the potential-decreasing part, there is now a sole new peak which corresponds with the $Au^{III}(OH)_3/Au^0$ equilibrium for the three Au-richest post-solder alloys, and with the Ag^{I}_2O/Ag^0 equilibrium for LFWG which contains less gold but more silver.

Galvanic Coupling of a Parent Alloy and its Post-Solder Alloy

Galvanic corrosion experiments were carried out for about two hours with following both the common potential and the exchange current between coupled alloy and post-solder. Two examples of the obtained curves are given in Fig. (**4**) while the average values of the potential of the parent alloy and its post-solder alloy together, and the current recorded between the two, are given in Table **5**.

Generally the potential evolves over the immersion duration, with first an increase followed by a decrease. Its average value over the experiment is generally comprised between the two E_{ocp} potentials which were separately measured on the first part of the cyclic polarization curves of the parent alloy and of the post-solder alloy. The exchange current, which is divided by the anodic surface, is more or less important, and can be close to the micro-ampere by cm². Its negative values show that, in most cases, it is the parent alloy that plays the role of anode and then is more corroded because of the coupling with the post-solder alloy. This is generally consistent with the order of E_{ocp} potential measured in the first parts of cyclic polarization.

DISCUSSION

The free potentials recorded for the High Noble and Noble parent alloys as well as for all the post-solder alloys which were studied here are always in the immunity domain of the precious elements belonging to the chemical composition. Then, the matrix, which contains the greatest part of gold, platinum, palladium and/or silver, is not exposed to corrosion. Concerning the other elements (Zn, In, Ga, Sn), the ones which are in solid solution in the matrix are not

Table 2.   High Noble Parent Alloys: Values of the Free Potential Over 2 Hours and of E_{ocp} During the Two Parts of the Cyclic Polarization; Situation in the Pourbaix Diagrams of the Main Elements Belonging to the Chemical Composition of the Alloys

E /NHE (mV)	t = 0	t = 30'	t = 1h	t=1h30'	t = 2h	PC ↑	PC ↓
dSIGN98(HN)	**+175**	**+135**	**+129**	**+126**	**+127**	**+120**	**+1009**
86%Au	*Au (immunity)*						Au^0/Au^{III}
12%Pt	*Pt (immunity)*						PtO_2
2%Zn	$Zn(OH)_2$ (passivation)						
A. Hard (HN)	**+282**	**+336**	**+367**	**+383**	**+391**	**+326**	**+1065**
86%Au	*Au (immunity)*						Au^0/Au^{III}
9%Pt	*Pt (immunity)*						PtO_2
3%Pd	*Pd (immunity)*						$Pd(OH)_4$
1%In	In_2O_3 (passivation)						
dSIGN91(HN)	**+209**	**+188**	**+192**	**+197**	**+198**	**+190**	**Several Peaks**
60%Au	*Au (immunity)*						Au^0/Au^{III}
31%Pd	*Pd (immunity)*						$Pd(OH)_4$
8%In-1%Ga	In_2O_3 and Ga_2O_3 (passivation)						
Lodestar (HN)	**+349**	**+331**	**+318**	**+308**	**+300**	**+274**	**Several Peaks**
52%Au	*Au (immunity)*						Au^0/Au^{III}
39%Pd	*Pd (immunity)*						$Pd^{IV}/Pd^{II}/Pd^0$
9%In-2%Ga	In_2O_3 and Ga_2O_3 (passivation)						
W (HN)	**+185**	**+66**	**+71**	**+75**	**+74**	**+73**	**Several Peaks**
54%Au	*Au (immunity)*						Au^{III}/Au^0
26%Pd	*Pd (immunity)*						Pd^{IV}/Pd^{II}
16%Ag	*Ag (immunity)*						Ag^{II}/Ag^I
3%Sn-2%In	$Sn(OH)_4$ and In_2O_3 (passivation)						

directly exposed to the solution. On the contrary, when such elements belong to the dispersed precipitates when they exist, their oxidation is probably very limited since the free potential is always in their passivation domains. It is this same passivation phenomenon that elsewhere protected the Predominantly Base alloys since the free potential is in the passivation domains of Ni, Cr and W. For that ones, corrosion really occurs but is extremely low, because of the thin external passivation layer of oxides or hydroxides which initially formed in the case of Pisces Plus (may be especially due to WO_3 which perhaps accelerates passivation). The case of the 4ALL alloy is not so clear since oxidized Mo is present as ions and not as solid precipitates on the surface. This alloy probably finished its passivation during the cyclic polarization.

All the alloys, the main elements of which are in their immunity domain after immersion, displayed a high value of free potential, which is of the same level that the one which was preliminarily measured with a polished Pt counter electrode used as a working electrode. Then, the potential measured by all these electrodes was the potential of the solution, which is fixed by the redox equilibrium between water and dissolved oxygen. It can be noted that this potential was particularly low in the case of dSIGN59, i.e. the sole Noble

Pd-based alloy. The free potentials of the two PB alloys were sensibly lower than for the other alloys, probably because no element of their composition (notably their base elements) was in an immunity situation.

The cyclic polarization runs enhanced the differences of electrochemical behavior between the alloys. After having oxidized all the elements present during the potential-increasing part of the experiment, there was a sole peak {Au(OH)₃/Au} in the case of the alloys with the highest contents of gold (dSIGN98 and Aquarius Hard with their 86%Au), or with simultaneously a lower Au content and a significant Ag content (post-solder .585, .615 and .650). The peak can be obviously more in correspondence with the {Ag₂O/Ag} equilibrium when the silver content is important (post-solder LFWG 27%Ag), even if there is the double of gold content. When simultaneously the gold content is not very high and palladium is present with a high content, the potential-decreasing part of the polarization curve contains several peaks, which reveals the participation of more than one element to the oxidation-reduction reactions.

The galvanic corrosion experiments showed that the order of E_{ocp} potentials between a parent alloy and its post-solder led to a corrosion of the alloy with the lowest potential enhanced
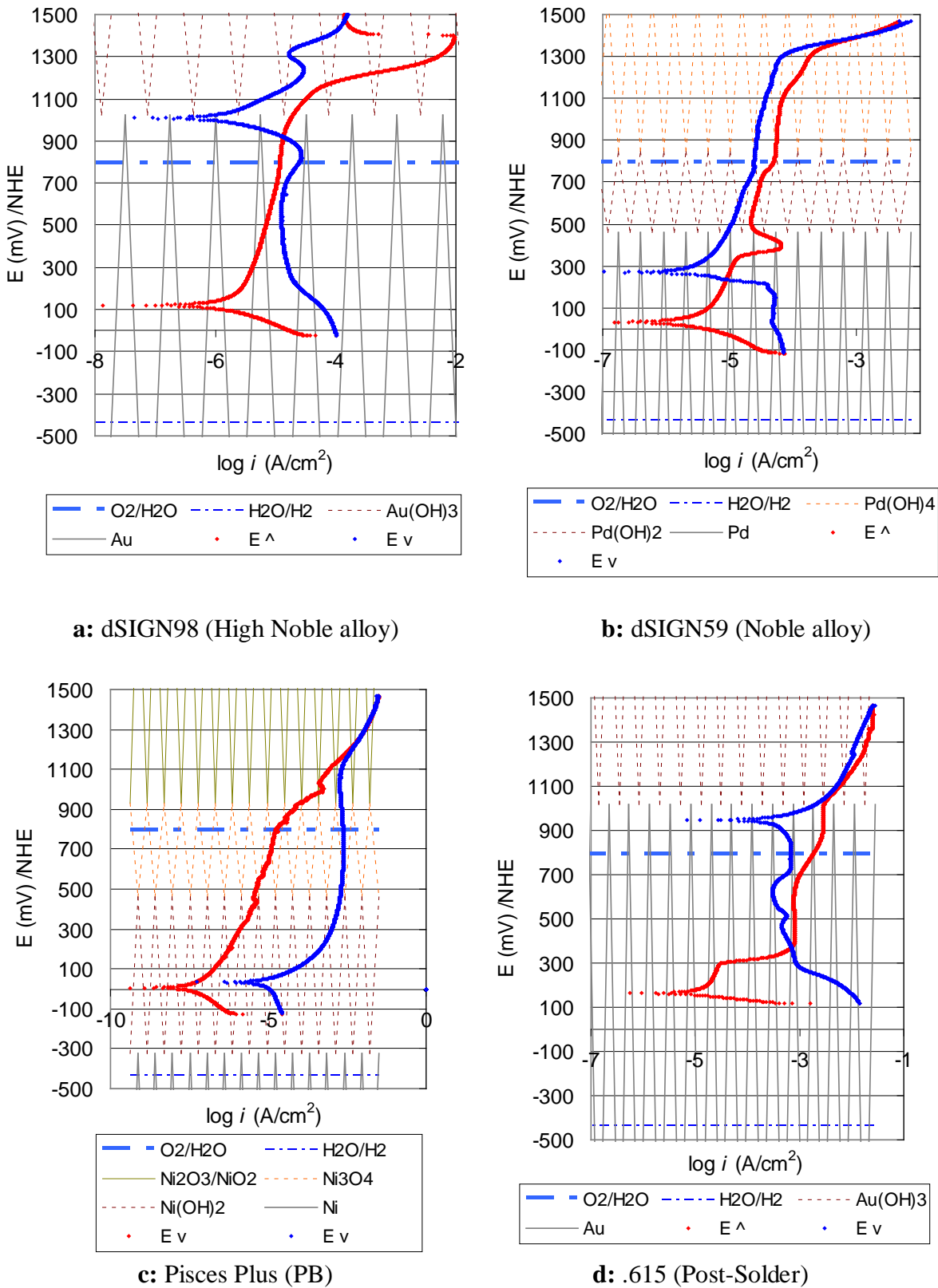
a: dSIGN98 (High Noble alloy)

b: dSIGN59 (Noble alloy)

c: Pisces Plus (PB)

d: .615 (Post-Solder)

Fig. (3). Typical cyclic polarization curves obtained for a range of alloys.

by coupling with the other alloy. Fortunately, the absolute value of the current decreases, probably because of the impoverishment of the solution in dissolved oxygen, which is also revealed by the decrease of the potential after a more or less long time. However, this galvanic corrosion can be maintained at a high level in case of discontinuous or continuous enrich-

ment in oxygen, like in real situation when saliva is present with a lower thickness along the framework. Fortunately, the post-solder alloy, which has the lowest surface exposed to the buccal milieu compared to the parent alloy, is often in a cathodic situation.

Table 3. Noble and PB Parent Alloys: Values of the Free Potential Over 2 Hours and of E_{ocp} During the Two Parts of the Cyclic Polarization; Situation in the Pourbaix Diagrams of the Main Elements Belonging to the Chemical Composition of the Alloys

E /NHE (mV)	t = 0	t = 30'	t = 1h	t=1h30'	t = 2h	PC ↑	PC ↓
dSIGN59 (N)	+40.5	+44.5	+38.5	+35.5	+33.5	+31.0	+268.8
59%Pd28%Ag				*Pd and Ag (immunity)*			
8%Sn-3%In-1%Zn				$Sn(OH)_4$, In_2O_3 and $Zn(OH)_2$ *(passivation)*			
4ALL (PB)	-61.5	-35.5	-45.5	-51.5	-51.5	-64.9	+206.6
61%Ni-26%Cr -11%Mo			$Ni(OH)_2$ and $Cr(OH)_3$ (passivation) and **MoO_4^{2-} (active state)**				
P.Plus (PB)	-73.5	+25.5	+40.5	+32.5	+27.5	+ 5.7	+ 33.6
62%Ni-22%Cr -11%W				$Ni(OH)_2$, $(Cr(OH)_3$ and WO_3 *(passivation)*			

Table 4. Post-Solder Alloys: Values of the Free Potential Over 2 Hours and of E_{ocp} During the Two Parts of the Cyclic Polarization; Situation in the Pourbaix Diagrams of the Main Elements Belonging to the Chemical Composition of the Alloys

E /NHE (mV)	t = 0	t = 30'	t = 1h	t=1h30'	t = 2h	PC ↑	PC ↓
.585	+279	+281	+277	+276	+275	+251	+883
59%Au				*Au (immunity)*			Au^{III}/Au^0
16%Ag				*Ag (immunity)*			AgO /Ag_2O
18%Cu				Cu_2O / $Cu(OH)_2$			$Cu(OH)_2$
7%Ga				Ga_2O_3			
.615	+283	+284	+281	+277	+270	+164	+947
61%Au				*Au (immunity)*			Au^{III}/Au^0
13%Ag				*Ag (immunity)*			Ag_2O/AgO
17%Cu				Cu_2O / $Cu(OH)_2$			$Cu(OH)_2$
8%In				In_2O_3			
.650	+283	+287	+285	+287	+287	+256	+1045
65%Au				*Au (immunity)*			Au^{III}/Au^0
13%Ag				*Ag (immunity)*			$Ag^{III}/Ag^{II}/ Ag^I$
20%Cu				Cu_2O / $Cu(OH)_2$			$Cu(OH)_2$
2%Ga				Ga_2O_3			
LFWG	+277	+279	+277	+275	+274	+182	+730
56%Au				*Au (immunity)*			
27%Ag				*Ag (immunity)*			Ag_2O/Ag^0
16%Zn				$Zn(OH)_2$			

To finish, one can remark that a part of these results can be compared to results previously obtained in the same electrolyte for other alloys having similar chemical compositions, with generally a good agreement. For example, the levels of free potentials measured for the dSIGN98, dSIGN91 and the 4ALL are consistent with results previously obtained on a (85Au-12Pt)-base alloy, a (62Au-29Pd)-base alloy and a (65Ni-26Cr-6Mo)-base alloy (all contents in wt.%) in a similar electrolyte [9] (water, 0.9%NaCl, 37°C). In the same solution, it is also the case for dSIGN59 and a 75Pd-6Ag-6Au-6In alloy [10] e.g. with a chemical composition of the same type (but slightly different), and for the Lodestar alloy and an alloy which has exactly the same chemical composition [11]. In the case of the latter work, in which cyclic polarization curves were performed as here, the potential-decreasing part displayed also a new E(I=0) potential systematically higher than the one of the potential-increasing part, for several alloys and several different solutions. In some cases
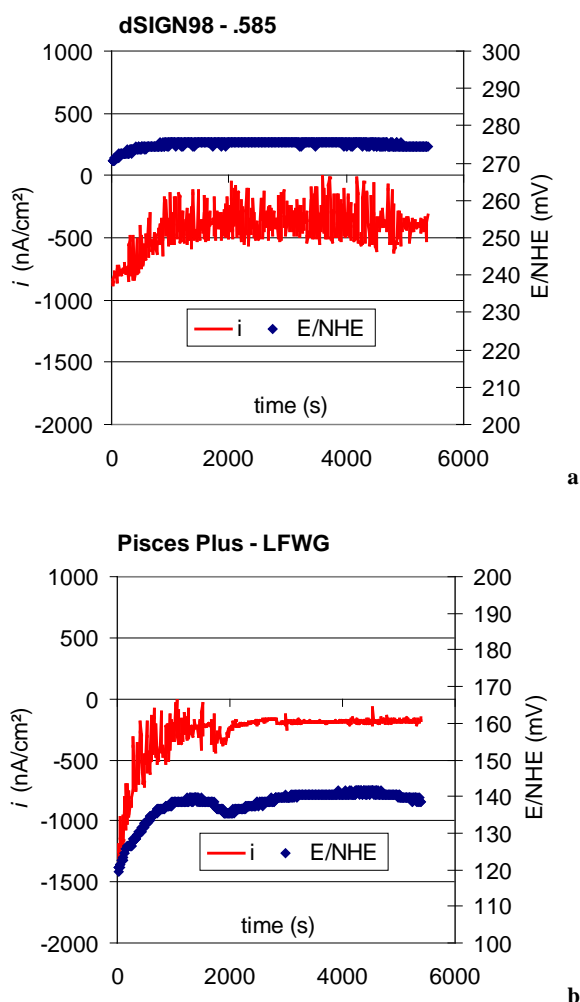
dSIGN98 - .585

a

Pisces Plus - LFWG

b

Fig. (4). Two examples of galvanic corrosion results. (**a**) a HN alloy and (**b**) a PB alloy.

Table 5.   **Average Values Over 2 Hours of the Common Potentials and Exchange Current Densities for the Different {Parent Alloy <-> Post-Solder Alloy} Couplings**

Parent - Post Solder	E (mV)	I/S (nA/cm²)	Corroded Alloy
dSIGN98 - .585	+275	-416	dSIGN98
Aquarius Hard - .650	+282	23	.650
dSIGN91 - 615	+262	-165	dSIGN91
Lodestar - .615	+236	-10	Lodestar
W - LFWG	+152	-1238	W
dSIGN59 - .615	+54	-2420	dSIGN59
4ALL - LFWG	+101	-652	4ALL
Pisces Plus - LFWG	+138	-276	Pisces Plus

the existence of several peaks in the potential-decreasing part was also observed and interpreted as being a complex oxida-

tion behavior of the alloy. Here these were further explained by using the Pourbaix's diagrams of the elements belonging to the alloy's chemical compositions.

CONCLUSION

Despite their differences of chemical compositions most of the precious metal-based parent alloys and post-solder alloys cannot be significantly corroded when they are in contact with a neutral NaCl-containing aqueous solution. The oxidation of their constitutive elements, even of the noblest ones, is possible with significant corrosion rates only if high values of electrical potential are applied, which cannot be really achieved by the strongest oxidant that can exist in such a solution (dissolved O_2). On the contrary, the less expensive PB alloys, which are protected against corrosion only by a passivation layer, are slowly corroded. However, a galvanic corrosion can occur when a parent alloy and its usual post-solder are coupled. Fortunately, it is the alloy with the more important surface that plays the role of anode, i.e. would be corroded by galvanic coupling, with very limited consequences for the mechanical resistance of the framework.

ACKNOWLEDGEMENTS

REFERENCES

[1]   Schiffleger BE, Ziebert GJ, Dhuru VB, Brandtley WA, Sigaroudi K. Comparison of accuracy of multiunit one-piece castings. J Prosthet Dent 1985; 54: 770-6.

[2]   Ziebert GJ, Hurtado A, Glapa C, Schiffleger BE. Accuracy of one-piece castings, preceramic and postceramic soldering. J Prosthet Dent 1986; 55: 312-7.

[3]   Schluger S, Youdelis RA, Page RC, Johnson RH. Periodontal Deseases. Lea & Febiger: Philadelphia 1990.

[4]   Wictorin L, Fredrisson H. Microstructure of the solder-casting zone in bridges of dental gold alloys. Odontol Rev 1976; 27: 187-96.

[5]   Kriebel R, Moore BK, Goodacre CJ, Dykema RW. A comparison of the strength of base metal and gold solder joints. J Prosthet Dent 1984; 51: 60-6.

[6]   De March P, Berthod P. A metallographic study of several alloys and of their pre-solder and post-solder joints used in dental prostheses. Mater Sci Ind J 2008; 4: 297-305.

[7]   Sun D, Monaghan P, Brandtley WA, Johnston WM. Electrochemical impedance spectroscopy study of high-palladium dental alloys. Part II: behavior at active and passive potentials. J Mater Sci Mater Med 2002; 13: 443-8.

[8]   Pourbaix M. Atlas d'équilibres électrochimiques. Gauthier-Villars: Paris 1963.

[9]   Manaranche C, Hornberger H. A proposal for the classification of dental alloys according to their resistance to corrosion. Dent Mater 2007; 23: 1428-37.

[10]   Mueller WD, Schoepf C, Nascimento ML, *et al.* Electrochemical characterisation of dental alloys: its possibilities and limitations. Anal Bioanal Chem 2005; 381: 1520-5.

[11]   Sun D, Monaghan P, Brandtley WA, Johnston WM. Potentiodynamic polarization study of the *in vitro* corrosion behavior of 3 high-palladium alloys and a gold-palladium alloy in 5 media. J Prosthet Dent 2002; 87: 86-93.